Chinese Journal of
POLYMER SCIENCE

RESEARCH ARTICLE

https://doi.org/10.1007/s10118-025-3445-0
Chinese J. Polym. Sci. **2026**, *44*, 1760–1766

The Monitoring of Anisotropic Tracer Nanoparticles by Depolarized Dynamic Light Scattering for Micro-rheology with Improved Contrast and Accuracy

Bing-Hui Xue, Yuan Liu, and Pan-Chao Yin*

State Key Laboratory of Luminescent Materials and Devices & South China Advanced Institute for Soft Matter Science and Technology, Guangdong Basic Research Center of Excellence for Energy and Information Polymer Materials, South China University of Technology, Guangzhou 510641, China

Electronic Supplementary Information

Abstract Compared to mechanical rheology, micro-rheology (μR) can probe the viscoelasticity of soft matter non-invasively with spatial resolution and broad temporal coverage; however, the measurement quality is undermined by interference from the structural and dynamic inhomogeneity of the tested media. Herein, gold nanorods are dispersed in tested media as tracer particles, and their diffusive dynamics are monitored by depolarized dynamic light scattering for the analysis of the rheological properties of the tested media, as the rotational/translational dynamics of tracers can be converted to shear modulus *via* the generalized Stokes-Einstein relation. Because of their strong optical scattering to the laser and the polarization of incident light, the contrast in the dynamics of gold nanorods over the media can be enhanced, rendering the fast and accurate measurement of rheological properties. The method was verified for applications in broad types of substrates, including ergodic systems such as polymer solutions, silica suspensions, non-ergodic gel systems, and biological fluids such as plasma. The critical experimental parameters, for example, tracer size and scattering angle range, are studied for their impact on the measurement quality, and they can be systematically optimized for feasible and practical applications of the developed μR method.

Keywords Depolarized dynamic light scattering; Micro-rheology; Nanorod; Gels; Rotational dynamics

Citation: Xue, B. H.; Liu, Y.; Yin, P. C. The monitoring of anisotropic tracer nanoparticles by depolarized dynamic light scattering for micro-rheology with improved contrast and accuracy. *Chinese J. Polym. Sci.* **2026**, *44*, 1760–1766.

INTRODUCTION

The Brownian motion of tracers suspended in matrix has been applied to characterize the viscoelasticity of soft materials and microstructures through micro-rheology (μR) for more than two decades.[1–7] Video particle tracking (VPT) technique or light scattering methods have been employed to measure the translational diffusive motion for mean square displacement (MSD) and/or rotational diffusive motion for mean square angular displacement (MAD), and a generalized Stokes-Einstein relation (GSER) has been applied to convert the displacement to the frequency-dependent shear modulus, $G^*(\omega)$.[8–11] Compared to MAD, the measurement of the MSD of tracers is easier, but the obtained information is limited, especially for rheological properties at high frequency, since the translational motion of the probes can be quenched in strongly confined geometries.[5] To fulfill the detection of MAD, spherical tracer particles with internal optical anisotropy such as liquid crystal particle (LCP), was applied at first.[10] In comparison to LCP, tracer particles with anisotropic topologies, *e.g.*, gold nanorods (GNRs), have been broadly used since their sizes can be continuously modulated and their applications in systems at different length scales can be favored. The pioneering work by Crocker *et al.* has demonstrated the feasibility of deducing the shear modulus from the MAD of GNRs using VPT method;[12] nevertheless, it requires long time measurements to ensure the statistics of collected data and moreover, sophisticated data processing techniques. This not only lowers down the efficiency for μR measurements, but also severely limits its applications in systems under non-equilibrium state. For anisotropic particles, the off-diagonal elements of the polarizability tensor are not zero, which leads to the changing of the polarization and contributes a signal of depolarized scattering.[13] Since only the anisotropic tracer can contribute to the depolarized signal, the depolarized dynamic light scattering (DDLS) setup filters the possible interference originating from the scattering of the matrix. Therefore, the orientational correlation function can be measured by DDLS, which can overcome the above problems owing to the impact on the polarization of light and strong optical scattering of GNRs.

Herein, the rotational Brownian motion of GNRs is mea-

* Corresponding author, E-mail: yinpc@scut.edu.cn
Special Topic: Functional Gels
Received July 23, 2025; Accepted September 1, 2025; Published online December 22, 2025

sured employing DDLS, and the respective rod-based rotational GSER is also solved for the complex shear modulus in the Fourier frequency domain (Fig. 1). Benefitting from the orientation dependent surface plasmon resonance of GNRs, the scattered light is strongly polarized, which makes the DDLS measurement fast and accurate. Meanwhile, the polarizer in DDLS set-up filters out the signals of isotropic matrix, ensuring the high contrast and the purity of signal of the GNRs (Fig. 1c).[14,15] The newly developed μR method is also verified in various soft matter systems, including polymer solutions, silica suspensions, functional gels and biological tissues.

EXPERIMENTAL

The details of experimental section and complementary data are presented in the electronic supplementary information (ESI).

THEORY

The derivation of the GSER in the Fourier domain for the rotation of anisotropic tracers (rod) is presented, from which the shear modulus can be finally extracted. Typically, the rotation of a rod can be described by a generalized Langevin equation:

$$I_r\dot{\Omega}(t) = f_R(t) - \int_0^t \zeta_r(t-\tau)\,\Omega(\tau)\,d\tau$$
$$\Omega(t) = \frac{d\theta}{dt} \quad (1)$$

where I_r and $\Omega(t)$ are the rotational inertia and angular velocity of the rod, respectively; the dot represents the time derivative. $\zeta_r(t)$ is the rotational memory function describing the local viscoelasticity of the isotropic, incompressible continuum without local heterogeneities and neglects finite-size effects.[4] The random thermal driving torque $f_R(t)$ covers both instantaneous and reactive stochastic forces and it follows a Gaussian distribution, which makes $f_R(t)$ decouple from the distribution of velocities:

$$\langle\Omega(0)\,f_R(t)\rangle = 0 \quad (2)$$

where the brackets correspond to ensemble average.

The solution of Eq. (1) is similar to that for the translational Langevin equation. Taking the Fourier transform of Eq. (1) gives us:

$$\mathcal{F}[\Omega(t)] = \frac{\mathcal{F}[f_R(t)] + I_r\Omega(0)}{i\omega I_r + \mathcal{F}[\zeta_r(t)]} \quad (3)$$

where Eq. (3) is simplified using the convolution theorem: $\mathcal{F}\left[\int_0^t d\tau\Omega(\tau)\,\zeta_r(t-\tau)\right] = \mathcal{F}[\zeta_r(t)]\,\mathcal{F}[\Omega(t)]$, and $\omega = \frac{1}{t}$. We multiply Eq. (3) by $\Omega(0)$ and perform the ensemble averaging:

$$\mathcal{F}[\langle\Omega(0)\,\Omega(t)\rangle] = \frac{\mathcal{F}[\langle f_R(t)\,\Omega(0)\rangle] + \langle I_r\Omega(0)\,\Omega(0)\rangle}{\mathcal{F}[\zeta_r(t)] + i\omega I_r} \quad (4)$$

The thermal energy equipartition theorem exports the kinetic energy:

$$I_r\langle\Omega(0)\,\Omega(0)\rangle = k_BT \quad (5)$$

where k_B is the Boltzmann constant, T is the absolute temperature.

Together with the property of causality of $f_R(t)$ in Eq. (2), Eq. (4) can be further simplified as:

$$\mathcal{F}[\langle\Omega(0)\,\Omega(t)\rangle] = \frac{k_BT}{\mathcal{F}[\zeta_r(t)]} \quad (6)$$

where the initial term originating from the rotation inertia is negligible, except at very high frequency, and can be omitted. The above approximation is suitable, as suggested by previous studies and the subsequent experiments in this study.[1,12] The Fourier transform of the rotational memory function of rod can be described as follows:

$$\mathcal{F}[\zeta_r(t)] = \frac{\frac{1}{3}\pi L^3\mathcal{F}[\eta(t)]}{[\ln(p) + C_r]} \quad (7)$$

where L represents the rod length, $p = \frac{L}{d}$ is the length-diameter ratio of the rod, d is the diameter, $\mathcal{F}[\eta(t)]$ is the Fourier transformed viscosity, which is frequency dependent, and $C_r = -0.662 + \frac{0.917}{p} - \frac{0.05}{p^2}$, which is introduced to deal with

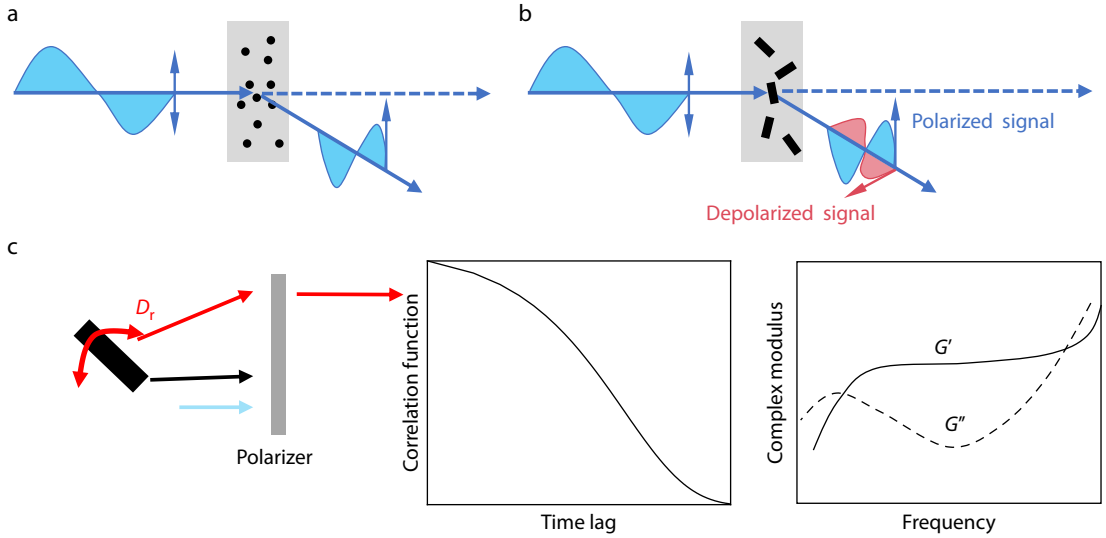

Fig. 1 Graphical representation of (a) ordinary dynamic light scattering and (b) depolarized dynamic light scattering; (c) Graphical representation of the detection of depolarized signals and the principle of achieving shear modulus.

the end effect of non-ideal rod with finite length. The expression for C_r is strictly valid for rods with p=2–20 based on reported works, and the sizes of tracers used in this work can meet the requirement.[16]

Meanwhile, the relationship between MAD ($\langle\Delta\theta^2(t)\rangle$) and $\mathcal{F}[\langle\Omega(0)\Omega(t)\rangle]$ can be described as:

$$\mathcal{F}[\langle\Omega(0)\Omega(t)\rangle] = \frac{(i\omega)^2}{2}\mathcal{F}\left[\left\langle\Delta\theta^2(t)\right\rangle\right] \tag{8}$$

Combining Eqs. (6)–(8), we can get the equation below:

$$\mathcal{F}[\eta(t)] = \frac{6k_BT}{(i\omega)^2\pi L^3\mathcal{F}\left[\left\langle\Delta\theta^2(t)\right\rangle\right]}[\ln(p) + C_r] \tag{9}$$

We applied the Stokes relation here, assuming that the matrix around the tracer is a continuum, which is valid when the length scale of the tracer is much larger than the characteristic sizes of the matrix. Based on the same assumption, the frequency-dependent complex modulus ($G^*(\omega)$) can be calculated utilizing $G^*(\omega) = i\omega\mathcal{F}[\eta(t)]$:

$$G^*(\omega) = \frac{6k_BT}{i\omega\pi L^3\mathcal{F}\left[\left\langle\Delta\theta^2(t)\right\rangle\right]}[\ln(p) + C_r] \tag{10}$$

Eq. (10) is the generalization of the Stokes-Einstein equation in Fourier domain.

For the practical calculation of the modulus curve in the experiment, we took the method used by Mason *et al.* to avoid potential errors near the frequency extremes. The MAD is expanded locally around a specific frequency ω:

$$\left\langle\Delta\theta^2(t)\right\rangle \approx \left\langle\Delta\theta^2\left(\frac{1}{\omega}\right)\right\rangle(\omega t)^{a(\omega)}, a(\omega) = \left.\frac{\mathrm{d}\ln\left\langle\Delta\theta^2(t)\right\rangle}{\mathrm{d}\ln t}\right|_{t=\frac{1}{\omega}} \tag{11}$$

The Fourier transformation of Eq. (11) gives:

$$i\omega\mathcal{F}\left[\left\langle\Delta\theta^2(t)\right\rangle\right] \approx \left\langle\Delta\theta^2\left(\frac{1}{\omega}\right)\right\rangle\Gamma[1 + a(\omega)]\,i^{-a(\omega)} \tag{12}$$

where the gamma function can be well represented by $\Gamma[1+a] \approx 0.457(1+a)^2 - 1.36(1+a) + 1.9$.[17] Substituting Eq. (12) into Eq. (10) and the application of Euler's equation leads to the expression for complex modulus, storage modulus ($G'(\omega)$) and loss modulus ($G''(\omega)$):

$$G^*(\omega) = \frac{6k_BTe^{\frac{i\pi a(\omega)}{2}}}{\pi L^3\left\langle\Delta\theta^2\left(\frac{1}{\omega}\right)\right\rangle\Gamma[1 + a(\omega)]}[\ln(p) + C_r] \tag{13}$$

$$\begin{aligned} G'(\omega) &= |G^*(\omega)|\cos\left(\frac{\pi a(\omega)}{2}\right) \\ G''(\omega) &= |G^*(\omega)|\sin\left(\frac{\pi a(\omega)}{2}\right) \end{aligned} \tag{14}$$

Finally, we have reached the feasible equations for the calculation of modulus using MAD of rod-like tracers.

The MAD of the tracer can be obtained from the correlation function measured by the DDLS experiments, as follows:

$$\left\langle\Delta\theta^2(t)\right\rangle = \frac{2}{3\left(q_2^2 - q_1^2\right)}\ln\left|\frac{g_{1,VH}(q_2,t)^{q_1^2}}{g_{1,VH}(q_1,t)^{q_2^2}}\right| \tag{15}$$

where $g_{1,VH}(q,t)$ is the first-order correlation function measured by DDLS, $\left(q = \frac{4\pi n}{\lambda}\sin\left(\frac{\theta}{2}\right)\right)$ is the scattering vector describing the spatial scales of DDLS experiments, n is the refractive index of the solvent, λ is the wavelength of the incident laser and θ is the scattering angle. The method used here is based on classical dynamic light scattering theory using the Gaussian approximation, which is universal.[13,14] As shown in Eq. (15), two correlation functions measured at two different scattering angles are required for the rheological analysis, and the effect of the combination of scattering angles on the micro-rheology results is discussed in next section.

RESULTS AND DISCUSSION

All data presented here are collected on a 3D-DLS Spectrometer (LS instruments, Switzerland) and the wavelength of laser is 660 nm. Two kinds of tracer GNRs with different dimensions are used to perform the experiments, which are NR170 (170 × 45 nm) and NR230 (230 × 15 nm), and the structure parameters of these rods have been confirmed from DDLS, small angel X-ray scattering (SAXS) and TEM (transmission electron microscopy) (Fig. S1 and Table S1 in ESI). The detailed description of the preparation of samples and experimental setup are covered in ESI. The obtained data are analyzed using the protocols clarified above, and the combination of scattering angles for these data are 60° and 130°. To validate the precision and robustness of the developed methodology, we have executed a series of control experiments on both nonergodic and ergodic systems. Furthermore, the key experimental parameters, including the tracer size and the combination of scattering angles, are explored for optimized measurement quality of the developed μR techniques.

The model system of functional gel, TPEG (tetra-polyethylene glycol, M_w=4.0×10^4 g/mol), is applied as non-ergodic systems for μR studies. For non-ergodic systems, the time-averaged quantities couldn't be consistent with ensemble-averaged quantities. Pusey and co-workers developed a method to acquire the ensemble-averaged first-order correlation function $g_{1,E}(q,t)$ based on time-averaged correlation functions of a sub-ensemble.[18,19] The specific expression is shown below:

$$g_{1,E}(q,t) = 1 + \frac{1}{Y}\left[\sqrt{g_2(q,t) - \sigma_T^2} - 1\right] \tag{16}$$

where $Y = \langle I(q)\rangle_E/\langle I(q)\rangle_T$. $\langle I(q)\rangle_E$ is the ensemble-averaged scattering intensity measured from the time-averaged scattering intensity while rotating the sample (different sub-ensembles), and $\langle I(q)\rangle_T$ is the time-averaged scattered intensity measured similar to $\langle I(q)\rangle_E$ but keeping the sample at a fixed position. $g_2(q,t)$ is the second-order correlation function obtained from experiments. σ_T^2 is the mean-square intensity fluctuation ($\sigma_T^2 = \frac{\left\langle I^2(q)\right\rangle_T}{\langle I(q)\rangle_T^2} - 1$), which is the same as the intercept of $g_2(q,t) - 1$. After acquiring the precise ensemble-averaged correlation function based on the protocols introduced above, the complex moduli of TPEG hydrogel can be calculated. As shown in Fig. 2(a), a plateau can be observed in the storage modulus, which is the feature of viscoelastic hydrogels, indicating that the size of NR170 tracer is larger than the mesh size of TPEG gel (about 20 nm).[14] At high frequencies, a scaling of $\omega^{\frac{1}{2}}$ corresponding to Rouse dynamics can be observed, which is a common phenomenon in neutral hydrogel systems.[20] Besides, we found reasonable agreement between mechanical rheology and the developed method for TPEG hydrogel (Fig. S2a in ESI),

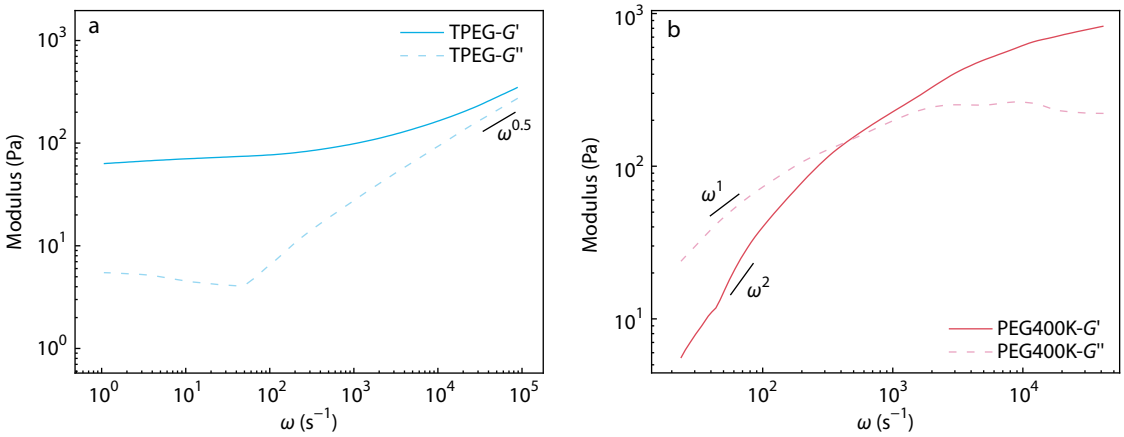

Fig. 2 The complex moduli of (a) non-ergodic system of TPEG hydrogel, (b) ergodic system of solution of PEG.

which further demonstrates the reliability of the μR method. The excellent characterization of TPEG gel demonstrates the robustness of the method developed. However, there are limitations to DDLS/anisotropic tracer based μR technology, as the fluctuation of tracer will be restricted due to its less discernible displacement within highly elastic matrix, and such fluctuation cannot be captured by the correlation function. As a result, the DDLS/anisotropic tracer based μR is suitable for material with low modulus instead of systems with high stiffness. Since the method is applied to non-ideal systems, and such applications are significant for practical use, some important points should be mentioned. To fulfill the assumptions of the method, the tracer size must be larger than the characteristic size of the matrix. For gel-like systems, there are two problems. One is the non-ergodicity, the valid micro-rheology experiment requires careful correction of non-ergodicity as we have illustrated above. The other one is the heterogeneity of the gel itself. As we all know, most of the gel systems are heterogeneous, and the heterogeneity of gel may affect the results of micro-rheology, leading to serious deviations. If the tracer particles are loaded after gelation, the tracer particle can not enter heterogeneities of aggregates of strands, and the results will be unreliable. Therefore, the tracer particle should be loaded *in situ* of the formation of gel, and the averaged dynamics of tracer can be monitored to rebuild the real rheological curve.

Compared with non-ergodic systems, the characterization of ergodic systems is more straightforward and feasible. Take the solution of PEG 400k (22.5 mg/mL) as an example, the mesh size (ξ) of the system is about 1.5 nm according to $\xi = R_g\left(\frac{C^*}{C}\right)^{0.75}$.[21] As shown in Fig. 2(b), the obtained complex moduli exhibit scaling of ω^1 and ω^2 at low frequencies, which are typical in polymer systems based on classical polymer physics theory. Then, the cross point of G' and G'' represents the terminal relaxation of the PEG chain.[20,22,23] We also performed the comparison between mechanical rheology and the developed method for this sample, and the obtained trends are the same but the data property of mechanical rheology is poor compared to the method developed (Fig. S2b in ESI), which demonstrates the reliability of the developed micro-rheology method and its important complementary effect to mechanical rheometer.

In addition to classical polymer systems, we also conducted experiments on colloidal particle systems. A suspension of 45 wt% of silica nanospheres with 32 nm diameter is measured (Fig. S1 and Table. S1 in ESI), and the obtained result is shown in Fig. 3(a). Different from polymer solutions, the scaling of complex moduli at low frequencies are 1, which is similar to other granular systems.[24–27] The above precise experimental results of various systems and the respective comparison between mechanical rheology demonstrate that micro-rheology based on DDLS and anisotropic tracer is capable of characterizing soft matter systems of interest with improved contrast and accuracy.

In the next section, we mainly discuss about the critical experimental parameters that control the experimental measurement quality of μR technology. As shown in the theory section (Eq. 15), a complete calculation of complex moduli requires the collection of correlation functions at least at two different scattering angles, and the specific combination could affect the results. The tracer MAD extracted from correlation functions measured at a series of combinations of scattering angles are shown in Fig. 3(b). The broad scattering angle coverage is required for the wide frequency window of rheological data just as suggested in Eq. (15). However, the collimation of commercialized equipment is restricted and the non-negligible diameter of laser beam will further compress the angle coverage. As a result, the choice of combination of scattering angles should consider the intrinsic property of the equipment. The combination of scattering angle 60°–130° used in this work is appropriate for most of the commercialized instruments.

The tracer size is another determining factor for the experimental coverage of μR frequency. As shown in Fig. 3(c), a little bit of deviation between two curves can be observed, while we wish to emphasize that this level of dispersion is within the expected variability for micro-rheology measurements, especially when comparing the results obtained with different tracer sizes, as the CTAB layer on the surface of NR170 and NR230 may have slight differences that affect the interaction between the matrix and tracer. Critically, the key rheological features such as the crossover frequency, slope in the terminal region and the overall order of magnitude of moduli show excellent consistency across the different tracer sizes. This robust agreement is the primary validation sought in consistency checks using different probe sizes. On the oth-

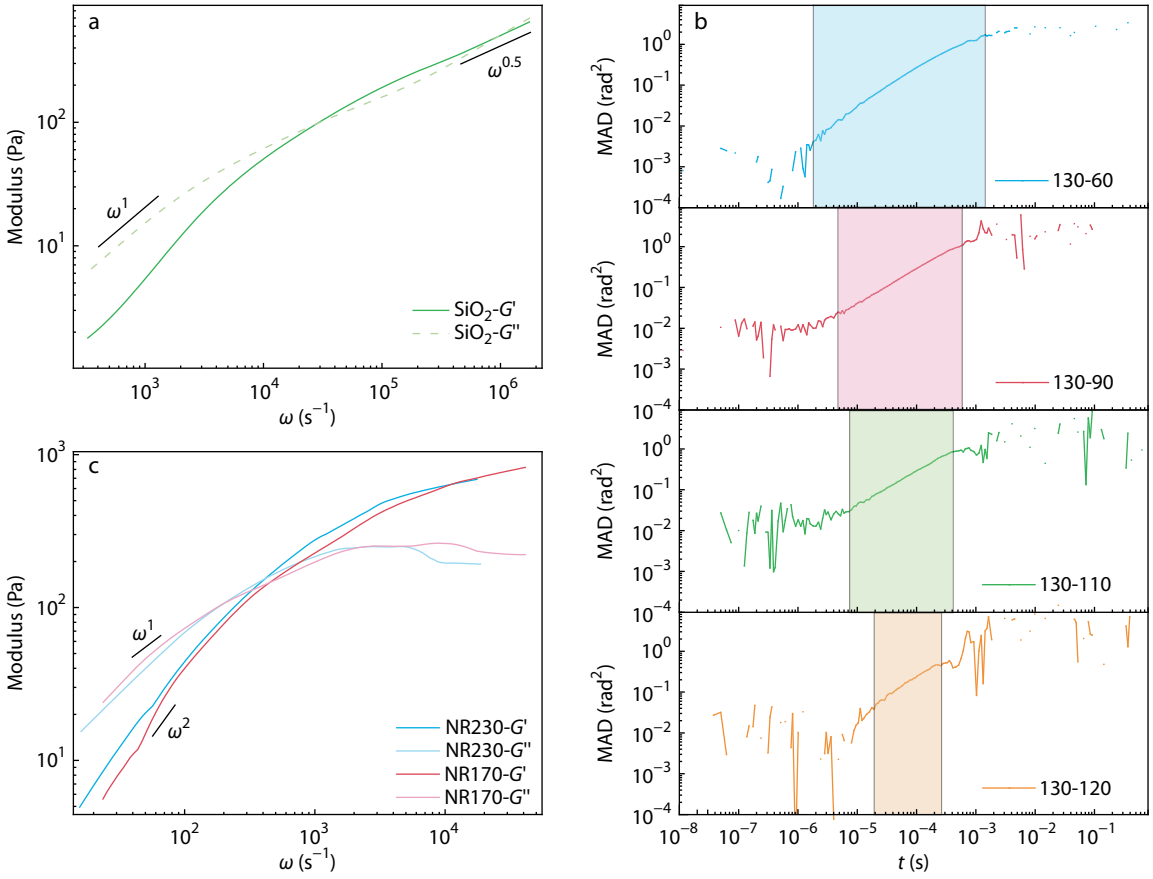

Fig. 3 The rheological results. (a) The complex moduli of suspension of silica nanospheres; (b) The MAD extracted from the correlation functions with different combinations of scattering angles, and the colored squares represent the temporal range within which the data is effective; (c) The complex moduli of PEG 400k solution using tracers with different sizes (NR170 and NR230).

er hand, this level of consistency is comparable to the deviation of other reported results.[11] Therefore, the data successfully demonstrates that the self-consistency shown in Fig. 3(c) is scientifically satisfactory and validates the reliability of the developed microrheology method. For larger tracers, the decay of the correlation function starts at longer times, which leads to a broader range of frequencies. However, it may cause potential sacrifice for high frequency region data, as the relaxation of larger tracers can be suppressed more severely, even if for rotational dynamics (Fig. 3c). Meanwhile, the homogeneous and stable suspension of tracers within matrix during experiment impose limit on their largest size. The tracer size should be larger than the characteristic size of the matrix to fulfill the assumption of the theory of micro-rheology and avoid wrong results.[28,29] Thus, realistic and precise micro-rheology experiment requires balanced choice of tracer size.

To demonstrate the significance of our method in practical applications, a micro-rheology experiment has been conducted on mouse plasma, which shall be intriguing for biologists as the rheological understanding of plasma is important to blood healthy. Plasma, which accounts for over half of the blood's volume, is the extracellular matrix of blood. The composition of plasma is complex, including plasma proteins, electrolytes, nutrients, enzymes, hormones, cholesterol and large amount of water (90%–92%).[30,31] As shown in Fig. 4,

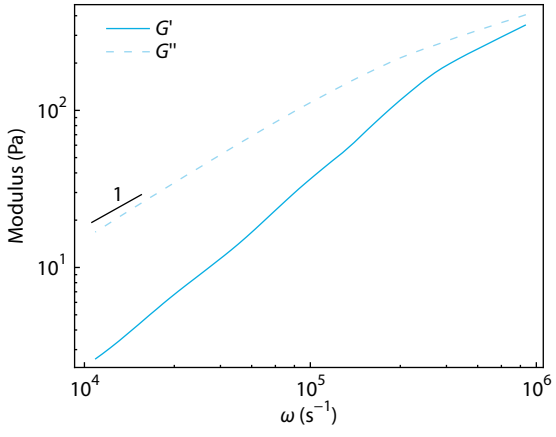

Fig. 4 The complex moduli of mouse plasma at room temperature.

the scaling of complex moduli at low frequency is close to 1, which is similar to the suspension of silica nanospheres (Fig. 3a). This similarity shall originate from the granular nature of plasma, and similar rheological results of plasma have also been reported by Deano *et al.*[32]

Compared with the reported micro-rheology method based on translational dynamics, the newly developed method is a good complement. The main difference between

the applicability of MAD-micro-rheology and MSD-micro-rheology is that a more accurate modulus can be obtained using rotational dynamics (MAD) if the compressibility of the matrix is unknown.[10] Besides, the dynamics of tracer is totally governed by the relaxation of matrix in micro-rheology, and the translational motion of tracer is severely restricted in matrix, especially for gels and other systems with relatively high modulus, which limits the acquiring of rheological data at high frequency. However, rotational motion only requires matrix relaxation at small length scale, rendering its potential at high frequency.

CONCLUSIONS

The newly developed micro-rheology method based on DDLS and anisotropic tracers is applicable to a broad range of fields due to its advantages, including fast and accurate measurement, wide range of frequency and the circumvention of interference from the matrix, as demonstrated by our experiments. We have shown here the crucial factors affecting the results of micro-rheology, such as the tracer size and the combination of scattering angles, and the respective standard for the choice. Although the passive nature of the developed technique restricts its application in experiments of nonlinear effects, the nondestructive nature contributes to its utilization in experiments of in situ monitoring and delicate biological systems, such as the characterization of mouse plasma. Besides, the technique is easy to set up with the combination of high-performance polarizers and multi-angle DLS instruments which is common for soft matter researchers. We believe that the developed method can be helpful to the field of biomaterials and soft matter considering its fast speed and accuracy.

Conflict of Interests

The authors declare no interest conflict.

Electronic Supplementary Information

Electronic supplementary information (ESI) is available free of charge in the online version of this article at http://doi.org/10.1007/s10118-025-3445-0.

Data Availability Statement

The data that support the findings of this study are available in the paper, or from the corresponding author.

ACKNOWLEDGMENTS

We thank the Shanghai Synchrotron Radiation Facility of BL10U1 (https://cstr.cn/31124.02.SSRF.BL10U1) for the assistance on SAXS measurements. This work was financially supported by the National Natural Science Foundation of China (Nos. 22241501 and 92261117), the Guangdong-Hong Kong-Macao Joint Laboratory for Neutron Scattering Science and Technology, the Open Fund of the China Spallation Neutron Source Songshan Lake Science City (No. DG24313519), and TCL science and technology innovation fund.

REFERENCES

1 Mason, T. G., Weitz, D. A. Optical measurements of frequency-dependent linear viscoelastic moduli of complex fluids. *Phys. Rev. Lett.* **1995**, *74*, 1250–1253.
2 Pine, D. J., Weitz, D. A., Chaikin, P. M., Herbolzheimer, E. Diffusing wave spectroscopy. *Phys. Rev. Lett.* **1988**, *60*, 1134–1137.
3 Dasgupta, B. R., Tee, S. Y., Crocker, J. C., Frisken, B. J., Weitz, D. A. Microrheology of polyethylene oxide using diffusing wave spectroscopy and single scattering. *Phys. Rev. E* **2002**, *65*, 051505.
4 Cheng, Z., Mason, T. G. Rotational diffusion microrheology. *Phys. Rev. Lett.* **2003**, *90*, 018304.
5 Andablo-Reyes, E., Díaz-Leyva, P., Arauz-Lara, J. L. Microrheology from rotational diffusion of colloidal particles. *Phys. Rev. Lett.* **2005**, *94*, 106001.
6 Qazvini, N. T., Bolisetty, S., Adamcik, J., Mezzenga, R. Self-healing fish gelatin/sodium montmorillonite biohybrid coacervates: structural and rheological characterization. *Biomacromolecules* **2012**, *13*, 2136–2147.
7 Berret, J. F. Local viscoelasticity of living cells measured by rotational magnetic spectroscopy. *Nat. Commun.* **2016**, *7*, 10134.
8 Squires, T. M., Mason, T. G. Fluid mechanics of microrheology. *Annual Review of Fluid Mechanics* **2010**, *42*, 413–438.
9 Schmidt, R. F., Kiefer, H., Dalgliesh, R., Gradzielski, M., Netz, R. R. Nanoscopic interfacial hydrogel viscoelasticity revealed from comparison of macroscopic and microscopic rheology. *Nano Lett.* **2024**, *24*, 4758–4765.
10 Gutiérrez-Sosa, C., Merino-González, A., Sánchez, R., Kozina, A., Díaz-Leyva, P. Microscopic viscoelasticity of polymer solutions and gels observed from translation and rotation of anisotropic colloid probes. *Macromolecules* **2018**, *51*, 9203–9212.
11 Cai, P. C., Krajina, B. A., Kratochvil, M. J., Zou, L., Zhu, A., Burgener, E. B., Bollyky, P. L., Milla, C. E., Webber, M. J., Spakowitz, A. J., Heilshorn, S. C. Dynamic light scattering microrheology for soft and living materials. *Soft Matter* **2021**, *17*, 1929–1939.
12 Molaei, M., Atefi, E., Crocker, J. C. Nanoscale rheology and anisotropic diffusion using single gold nanorod probes. *Phys. Rev. Lett.* **2018**, *120*, 118002.
13 Berne, B. J., Pecora, R. *Dynamic light scattering: With applications to chemistry, biology, and physics*. Dover, New York, **1976**.
14 Xue, B., Liu, Y., Tian, Y., Yin, P. The coupling of rotational and translational dynamics for rapid diffusion of nanorods in macromolecular networks. *Nat. Commun.* **2024**, *15*, 6502.
15 Balog, S., Rodriguez-Lorenzo, L., Monnier, C. A., Michen, B., Obiols-Rabasa, M., Casal-Dujat, L., Rothen-Rutishauser, B., Petri-Fink, A., Schurtenberger, P. Dynamic depolarized light scattering of small round plasmonic nanoparticles: when imperfection is only perfect. *J. Phys. Chem. C* **2014**, *118*, 17968–17974.
16 Ortega, A., García de la Torre, J. Hydrodynamic properties of rodlike and disklike particles in dilute solution. *J. Chem. Phys.* **2003**, *119*, 9914–9919.
17 Mason, T. G. Estimating the viscoelastic moduli of complex fluids using the generalized stokes-einstein equation. *Rheol Acta* **2000**, *39*, 371–378.
18 Pusey, P. N., Van Megan, W. Dynamic light scattering by non-ergodic media. *Phys. A* **1989**, *157*, 705–741.
19 Usuelli, M., Cao, Y., Bagnani, M., Handschin, S., Nyström, G., Mezzenga, R. Probing the structure of filamentous nonergodic gels by dynamic light scattering. *Macromolecules* **2020**, *53*, 5950–5956.
20 Rubinstein, M., Colby, R. H. *Polymer physics*. Oxford university press New York, **2003**.
21 Cooper, E. C., Johnson, P., Donald, A. M. Probe diffusion in

Graphical Abstract

The Monitoring of Anisotropic Tracer Nanoparticles by Depolarized Dynamic Light Scattering for Micro-rheology with Improved Contrast and Accuracy

Bing-Hui Xue, Yuan Liu, and Pan-Chao Yin

South China University of Technology

This study develops a micro-rheology method using gold nanorods as probes monitored *via* depolarized dynamic light scattering. It enables fast, accurate viscoelasticity measurements across diverse soft materials, from polymer solutions to biological fluids.

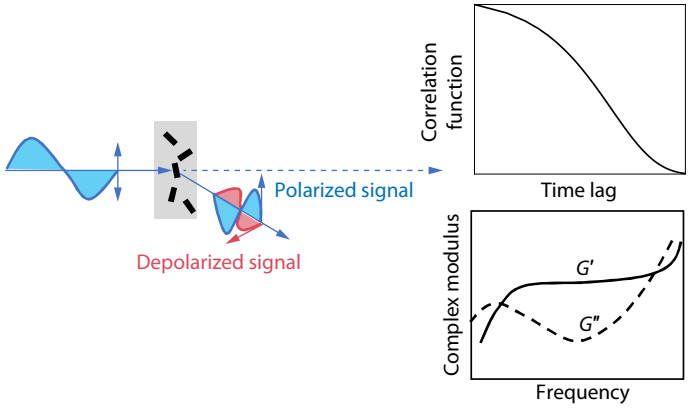

Chinese J. Polym. Sci. 2026, 44, 1760–1766 *https://doi.org/10.1007/s10118-025-3445-0*

polymer solutions in the dilute/semi dilute crossover regime: 1. poly(ethylene oxide). *Polymer* **1991**, *32*, 2815–2822.

22 Xue, B. H., Lai, Y. Y., Cai, L. K., Liu, Y., Yin, J. F., Yin, P. C. Emergent research trends on the structural relaxation dynamics of molecular clusters: from structure-property relationship to new function prediction. *Acc. Chem. Res.* **2024**, *57*, 3057–3067.

23 Matsumoto, A., Zhang, C., Scheffold, F., Shen, A. Q. Microrheological approach for probing the entanglement properties of polyelectrolyte solutions. *ACS Macro Lett.* **2021**, *11*, 84–90.

24 Xue, B., Liu, Y., Sun, W., Liang, Y., Yin, P. The spatiotemporal studies of the salt-hardening effect of the coacervates of nano-ions for aqueous super-ionic electrolytes with enhanced electrochemical stability. *J. Colloid Interface Sci.* **2025**, *696*, 137898.

25 Lai, Y. Y., Yang, J. S., Cai, L. K., Zhang, M. X., He, X. F., Yu, H. T., Li, M., Ning, G. H., Yin, P. C. Precise modulation of surface layer dynamics for tunable flowability and gas absorption properties of molecular porous liquids. *Adv. Funct. Mater.* **2023**, *33*, 2210122.

26 Xue, B., Lai, Y., Liu, Y., Li, M., Li, X., Yin, P. The counterion-mediated controllable coacervation of nano-ions with polyelectrolytes. *J. Colloid Interface Sci.* **2023**, *641*, 853–860.

27 Xue, B. H., Wei, L. F., Yin, J. F., Yang, J. S., Yin, P. C. Particle topology-regulated relaxation dynamics in cluster-ordering. *J. Chem. Phys.* **2024**, *160*, 154902.

28 Hess, M., Gratz, M., Remmer, H., Webers, S., Landers, J., Borin, D., Ludwig, F., Wende, H., Odenbach, S., Tschope, A., Schmidt, A. M. Scale-dependent particle diffusivity and apparent viscosity in polymer solutions as probed by dynamic magnetic nanorheology. *Soft Matter* **2020**, *16*, 7562–7575.

29 Krajina, B. A., Tropini, C., Zhu, A., DiGiacomo, P., Sonnenburg, J. L., Heilshorn, S. C., Spakowitz, A. J. Dynamic light scattering microrheology reveals multiscale viscoelasticity of polymer gels and precious biological materials. *ACS Cent. Sci.* **2017**, *3*, 1294–1303.

30 Brust, M., Schaefer, C., Doerr, R., Pan, L., Garcia, M., Arratia, P. E., Wagner, C. Rheology of human blood plasma: viscoelastic versus newtonian behavior. *Phys. Rev. Lett.* **2013**, *110*, 078305.

31 Beris, A. N., Horner, J. S., Jariwala, S., Armstrong, M. J., Wagner, N. J. Recent advances in blood rheology: a review. *Soft Matter* **2021**, *17*, 10591–10613.

32 Rodrigues, T., Mota, R., Gales, L., Campo-Deaño, L. Understanding the complex rheology of human blood plasma. *J. Rheol.* **2022**, *66*, 761–774.